ACS APPLIED MATERIALS & INTERFACES

RESEARCH ARTICLE

www.acsami.org

Grating-Coupled Surface Plasmon Enhanced Short-Circuit Current in Organic Thin-Film Photovoltaic Cells

Akira Baba,*[,†] Nobutaka Aoki,[‡] Kazunari Shinbo,[†,‡] Keizo Kato,[†,‡] and Futao Kaneko[†,‡]

[†]Center for Transdisciplinary Research, and [‡]Graduate School of Science and Technology, Niigata University, 8050 Ikarashi 2-nocho, Nishi-ku, Niigata 950-2181, Japan

ABSTRACT: In this study, we demonstrate the fabrication of grating-coupled surface plasmon resonance (SPR) enhanced organic thin-film photovoltaic cells and their improved photocurrent properties. The cell consists of a grating substrate/silver/P3HT:PCBM/PEDOT:PSS structure. Blu-ray disk recordable substrates are used as the diffraction grating substrates on which silver films are deposited by vacuum evaporation. P3HT:PCBM films are spin-coated on silver/grating substrates. Low conductivity PEDOT:PSS/PDADMAC layer-by-layer ultrathin films deposited on P3HT:PCBM films act as the hole transport layer, whereas high conductivity PEDOT:PSS films deposited by spin-coating act as the anode. SPR excitations are observed in the fabricated cells upon irradiation with white light. Up to a 2-fold increase in the short-circuit photocurrent is observed when the surface plasmon (SP) is excited on the silver gratings as compared to that without SP excitation. The finite-difference time-domain simulation indicates that the electric field in the P3HT:PCBM layer can be increased using the grating-coupled SP technique.

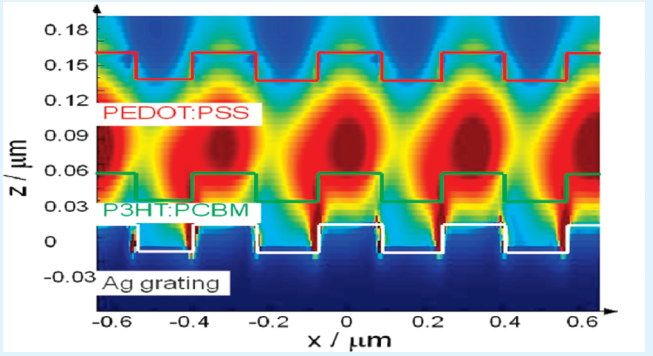

KEYWORDS: surface plasmon, grating structure, organic thin-film photovoltaic cell, short-circuit current, FDTD simulation

INTRODUCTION

Organic thin-film photovoltaic cells are one of the most promising candidates for inexpensive and flexible photovoltaic cells based on organic materials.[1,2] An important challenge in the advancement of the organic thin-film photovoltaic cells is reducing their film thickness while maintaining their high efficiency. Hence, it is essential to develop a way to strongly absorb light in the thin-film layer. Because surface plasmon resonance (SPR) offers an enhanced optical field, i.e., increased absorption in the cell, there has been considerable interest in fabricating plasmonic-structured photovoltaic cells.[3] The use of surface plasmons (SPs) in organic photovoltaic cells utilizing metal nanoparticles has been investigated as improved light absorption systems that provide high-efficiency cells.[4−6] The prism-coupling method has also been used for the improvement of the organic photovoltaic cell.[7−9] Although several SP-enhanced organic thin-film photovoltaic cells have been investigated to some extent with promising results,[10] there have been a few reports on grating-coupled SP-enhanced organic thin-film photovoltaic cells. In particular, few working organic photovoltaic devices with plasmonic grating structures have been reported, whereas several important studies using finite-difference time-domain (FDTD) simulations have been reported recently.[11,12] The grating-coupled technique is a prismless, convenient, propagating SPR excitation method.[13,14] There have been reports that light scattering and light trapping can be obtained on the grating surface (without SP excitation), resulting in the improvement of the obtained photocurrent.[15] Hence, in addition to the light scattering improvement effect, a remarkable improvement in the photocurrent of the cells might be obtained if the SP-enhanced field can be obtained on grating substrates. Recently, we demonstrated multimode SP excitations and enhanced photoluminescence properties of a metallic grating by using compact disk-recordable substrates.[16]

In this study, we demonstrate the fabrication of organic thin-film bulk-heterojunction photovoltaic cells on Blu-ray Disc recordable (BD-R) substrates for the excitation of grating-coupled SPs, which efficiently improve the photocurrent conversion. We also studied the distance dependence of the plasmon-enhanced photocurrent property by controlling the thickness of the P3HT:PCBM layer because the SP is an evanescent wave that exponentially decays as it moves away from the metal surface. Furthermore, in order to understand the experimental results, finite-difference time-domain simulations were performed by assuming that the organic thin-film photovoltaic cells had a grating structure. FDTD calculations indicated an increased electric field distribution in the cell, which corresponded well with the experimental results.

EXPERIMENTAL SECTION

Figure 1 depicts a schematic diagram of the fabricated bulk-heterojunction photovoltaic cell. The BD-R polycarbonate grating substrates were deposited with an ∼150-nm-thick silver layer by vacuum evaporation.

Received: March 11, 2011
Accepted: May 17, 2011
Published: May 17, 2011

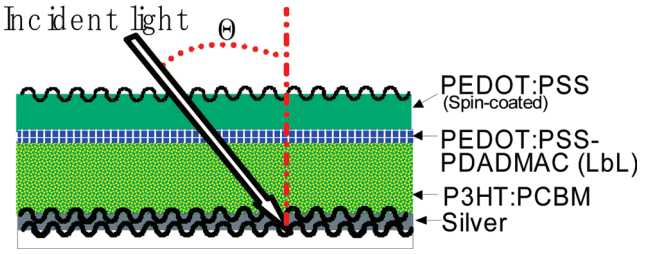

Figure 1. Schematic of the fabricated SPR-enhanced organic thin-film photovoltaic cell.

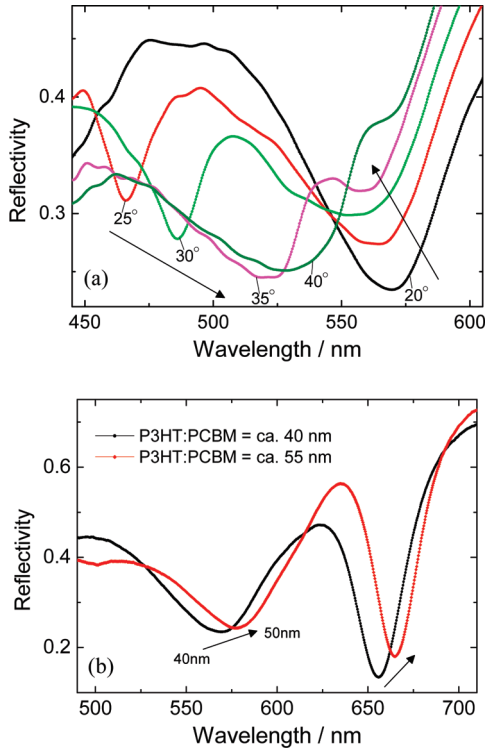

Figure 2. (a) SP reflectivity curves of the BD-R grating/silver (ca. 150 nm)/P3HT:PCBM film (ca. 40 nm)/10 bilayers of PEDOT:PSS-PDADMAC LbL film/PEDOT:PSS spin-coated film as a function of wavelength. (b) SP reflectivity curves of the BD-R grating/silver (ca. 150 nm)/P3HT:PCBM film (ca. 40 and 55 nm)/10 bilayers of PEDOT:PSS-PDADMAC LbL film/PEDOT:PSS spin-coated film at an incident light angle of 20°.

A procedure similar to the preparation technique reported in[17] was used to prepare the BD-R substrates. P3HT and PCBM were dissolved in trichloromethane with a P3HT:PCBM mass ratio of 1:1. The P3HT:PCBM thin film was deposited on silver/grating substrates by spin-coating the mixed solution at 2000 rpm for 1 min. The sample was then annealed at 100 °C for 1 h. Then, a multilayered film of low conductive PEDOT:PSS (conductivity = 1×10^{-5} S/cm) and poly(diallyldimethylammonium chloride) (PDADMAC),[17] which acted as a hole transport layer, was fabricated by the layer-by-layer (LbL) deposition technique.[18,19] The P3HT:PCBM surface samples were then alternately immersed in aqueous solutions of PEDOT:PSS and PDADMAC for 15 min each until a10 bilayers were obtained. Between consecutive immersions, the samples were rinsed twice using deionized water for a duration of 2 min. Finally, high conductivity PEDOT:PSS (conductivity = 150 S/cm) was deposited on the PEDOT:PSS/PSS LbL film by spin-coating at 3000 rpm for 1 min; this acted as the anode. The sample was then annealed at 100 °C for 30 min.

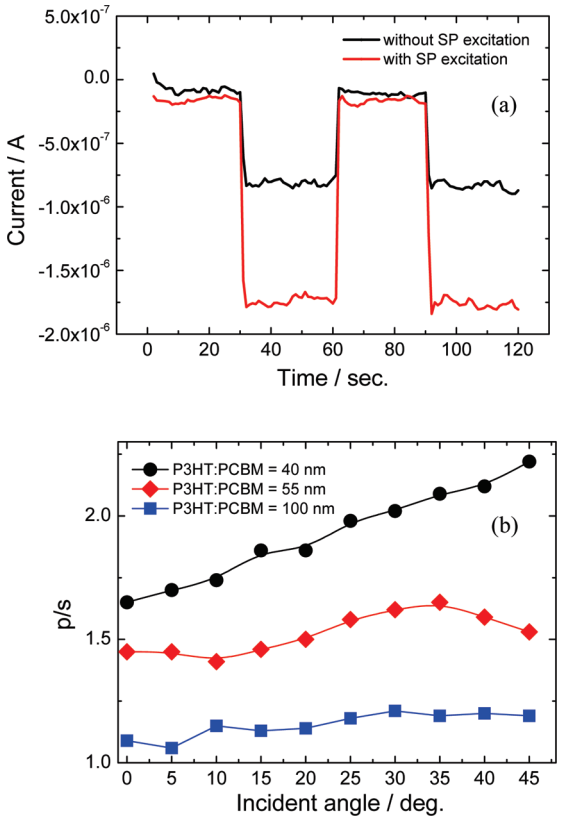

Figure 3. (a) Short-circuit photocurrent properties of the photovoltaic cell upon irradiation by visible light with SP excitation (p-polarization) and without SP excitation (s-polarization) (P3HT:PCBM = 40 nm). (b) Enhanced factor p/s, i.e., the ratio of the current with SP excitation (p-polarization) to the current without SP excitation (s-polarization).

RESULTS AND DISCUSSION

To study SP excitation properties of the fabricated cells, we measured the SPR reflectivity curves at fixed incident angles as a function of wavelength. The thickness of each layer was estimated by fitting the grating-coupled SPR experimental results (at 633 nm as a function of the incident angle) on the basis of a rigorous coupled-wave analysis (RCWA) method (G-Solver). Figure 2a shows the SPR reflectivity curves of the fabricated photovoltaic cells measured at fixed incident angles ranging from 20 to 45°. As shown in the figure, two resonance dips were observed for each angle, indicating that enhanced electric fields could be obtained in the cells. At an incident angle of 20°, dips were observed at approximately 430 and 540 nm. As the incident angle increased, the dip at 430 nm shifted toward higher wavelengths and the dip at 540 nm shifted toward shorter wavelengths. The resonance dips also shifted toward longer wavelengths when the thickness of the P3HT:PCBM films increased (Figure 2b), indicating that the P3HT:PCBM film existed within the SP-enhanced evanescent field region. The SP dip positions shifted closer to the UV−visible absorption peak of the P3HT:PCBM film, i.e., 520−560 nm.

To study the effect of SP excitation, we investigated the short-circuit photocurrent properties both with and without SP excitation. We performed photocurrent measurements by irradiating

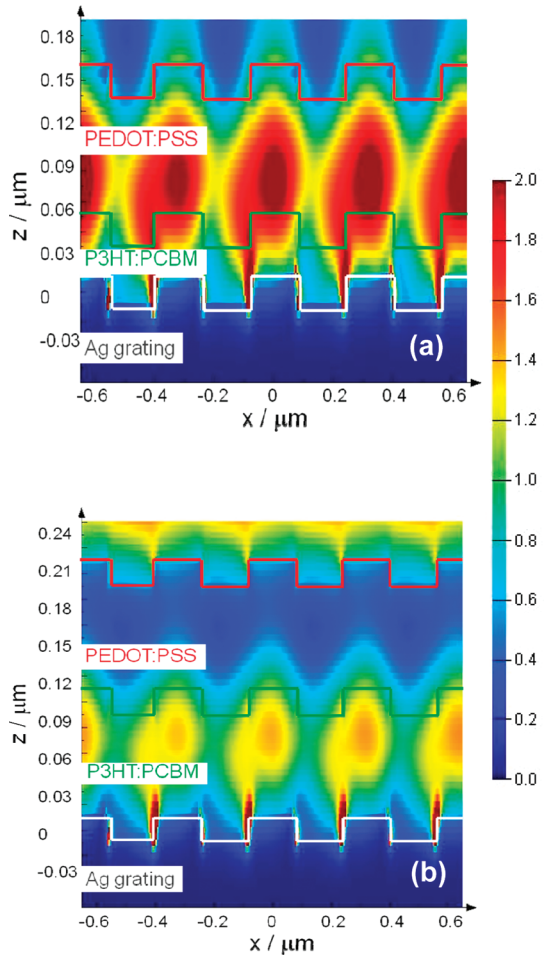

Figure 4. Electric field intensity map of the photovoltaic cell for different film thicknesses of the P3HT:PCBM layer (a) 40 and (b) 100 nm.

collimated visible light from a 350-mW xenon lamp. Figure 3a shows the short-circuit photocurrent properties of the fabricated organic photovoltaic cells in which the thickness of the P3HT:PCBM layer is approximately 40 nm. For SP excitation measurements, the sample was irradiated with p-polarized light, whereas for non-SP excitation measurements, the sample was irradiated with s-polarized light. As shown in Figure 3a, for all cases, the short-circuit current with SP excitation increased more compared with that without SP excitation. This result clearly indicates that the grating-coupled SP excitation can enhance the photoelectric conversion in the cell. The current for the grating-coupled SP excitation increased up to 2-fold more than that with no SP excitation. We plotted the enhanced factor p/s, i.e., the ratio of the current with SP excitation (p-polarization) to the current without SP excitation (s-polarization), as a function of the incident angle (Figure 3b) for each thickness of the P3HT:PCBM layer. It should be noted that the enhanced factor p/s increased with decreasing film thickness. Because the SP-enhanced optical field exponentially decayed as the distance from the silver surface increased, the increased current with the thinner P3HT:PCBM layer was caused by the stronger optical field in the wide range of the film. Furthermore, it should be noted that the short-circuit current increased at all incident angles, as exhibited by this plot. In all cases, the p/s factor was higher at higher incident angles, corresponding well with the results shown in Figure 2. It should be noted that the p/s factor obtained using BD-R grating substrates showed the highest enhancement among all the other grating pitches, which were measured using Compact Disc recordable (CD-R) (Λ = 1.6 μm) and Digital Versatile Disc recordable (DVD-R) (Λ = 740 nm) grating substrates.

For further studying the mechanism of the increased short-circuit current, we simulated the electric field of the photovoltaic cells by using the FDTD method. It has been reported that the increase in the electric field corresponds to the enhancement of absorption in the layer.[20] Figure 4 shows the electric field intensity map in the photovoltaic cells. In the simulations, we assumed a rectangular grating structure with a 320 nm grating pitch and a 20 nm grating depth. The incident angle of the irradiated light (λ = 550 nm) was 20°. We assumed two film thicknesses of the P3HT:PCBM layer: 40 and 100 nm. We also assumed the 100 nm PEDOT:PSS layer, as shown in Figure 4. In both cases, a strong electric field of more than 2-fold intensity compared with that of incident light was observed in the vicinity of the silver grating surface. The 40-nm-thick P3HT:PCBM layer existed within the strongly enhanced electric field region. On the other hand, the electric field intensity of the 100-nm-thick P3HT:PCBM layer decreased as compared to that seen in Figure 4a, although the electric field intensity was still enhanced up to 1.5 times more than that of incident light. This result obviously indicated that the SP excitation could increase the absorption of the irradiated light in the P3HT:PCBM layer. Hence, we obtained an increased short-circuit current wherein the amount of increase depended on the thickness of the P3HT:PCBM layer. Furthermore, the FDTD simulation corresponded well with the trend of the enhancement factor obtained from Figure 3, which depended on the P3HT:PCBM layer film thickness. As shown in maps a and b in Figure 5, for the case of the grating surface without SP excitation and with s-polarization irradiation, the electric field intensity in the cell was weaker than that for the case with SP excitation; this supported the experimental results. It should be noted that the electric field intensity without SP excitation of the grating structure was still enhanced in the cell as compared to that in the cell with a flat silver surface (without grating); this indicates that light scattering and trapping can be achieved on the grating surface even without SP excitation.[15] Hence, we can conclude that SP excitation can further increase the short-circuit current in addition to the enhancement by the light scattering effect on the grating structure.

Next, we measured the short-circuit photocurrent with and without SP excitation in the absorption region of the P3HT:PCBM film as a function of the wavelength of light irradiated on the film at an incident angle of 20° (Figure 6b). The SPR reflectivity curve measured at 20° is shown in Figure 6c for reference. For comparison, the UV−visible absorption spectrum of the spin-coated P3HT:PCBM film is shown in Figure 6a. As demonstrated in this figure, we again observed the increased photocurrent caused by the SP excitation. We should note that the enhanced photocurrent peak is close to one of the SPR dips, which is closer to the absorption peak wavelength of the P3HT:PCBM film. Figure 7 shows the corresponding incident photon to current conversion efficiency (IPCE) of the device with and without SP excitation. Although the efficiency is still low because of the unconventional device structure with the PEDOT:PSS anode, the IPCE with SP excitation is higher than that

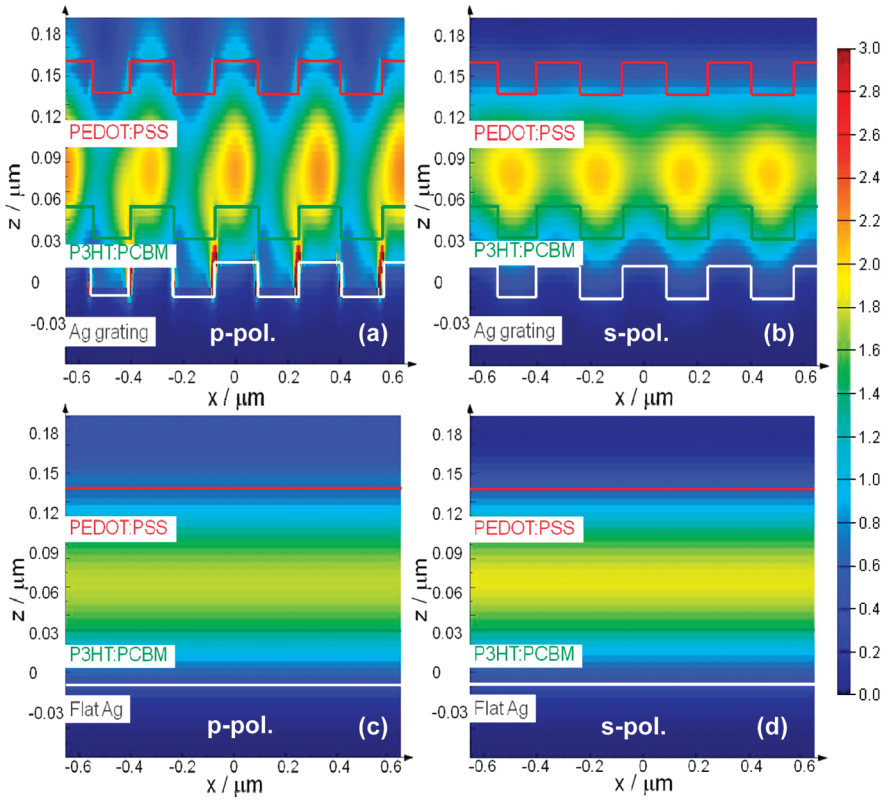

Figure 5. Electric field intensity map of the photovoltaic cell for (a) p-pol. (with SP excitation), (b) s-pol. (without SP excitation), (c) grating structure with p-pol., and (d) flat silver surface (no grating structure) with s-pol.

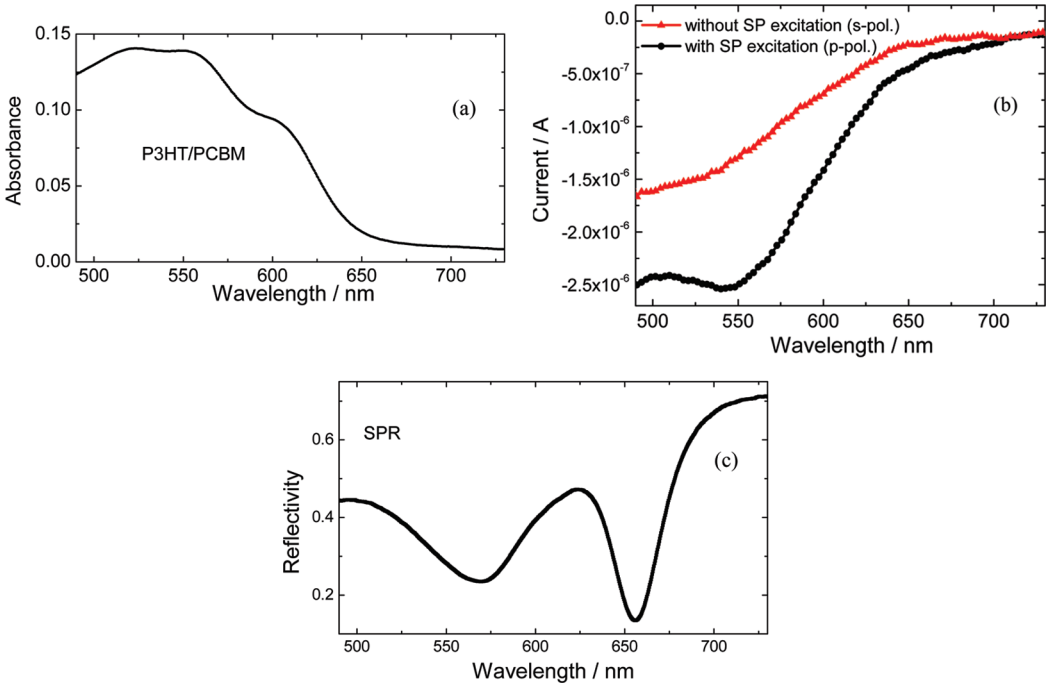

Figure 6. (a) UV−visible absorption spectrum of the P3HT:PCBM film, (b) Short-circuit photocurrent with and without SP excitation measured as a function of light wavelength at an incident angle of 20°, and (c) SPR reflectivity curve of the cell measured at 20°.

without SP excitation. This result clearly indicated that the SP excitation on the grating structure actually enhanced the device performance and was useful in improving organic thin-film photovoltaic cells.

dx.doi.org/10.1021/am200304x |*ACS Appl. Mater. Interfaces* 2011, 3, 2080–2084

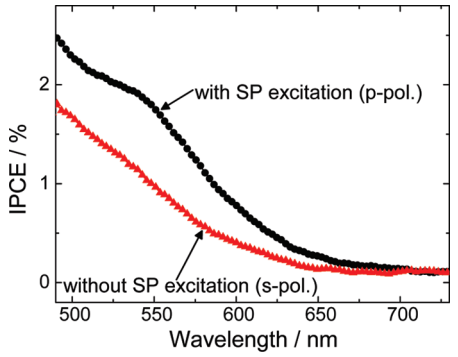

Figure 7. IPCE with and without SP excitation measured at an incident angle of 20°.

CONCLUSIONS

In conclusion, we have demonstrated the fabrication of grating-coupled SPR-enhanced organic thin-film photovoltaic cells and their improved short-circuit current properties. Obvious increases in the short-circuit photocurrent can be obtained when the propagating-SP is excited on the silver gratings as compared to that without SP excitation. The FDTD simulation indicates that the electric field in the P3HT:PCBM layer can be effectively increased using the grating-coupled SP technique. The demonstrated method should provide new opportunities to remarkably increase the efficiency of organic thin-film photovoltaic cells.

AUTHOR INFORMATION

Corresponding Author

*E-mail: ababa@eng.niigata-u.ac.jp.

ACKNOWLEDGMENT

This work was partly supported by the Adaptable and Seamless Technology transfer Program (A-STEP) from the Japan Science and Technology Agency (JST) and a Grant-in-Aid for Scientific Research from the Japan Society for the Promotion of Science.

REFERENCES

(1) Tang, C. W. *Appl. Phys. Lett.* **1986**, *48*, 183–185.
(2) Kim, J. Y.; Lee, K.; Coates, N. E.; Moses, D.; Nguyen, T. Q.; Dante, M.; Heeger, A. J. *Science* **2007**, *317*, 222–225.
(3) Atwater, H. A.; Polman, A. *Nat. Mater.* **2010**, *9*, 205–213.
(4) Kim, S. S.; Na, S. I.; Jo, J.; Kim, D. Y.; Nah, Y. C. *Appl. Phys. Lett.* **2008**, *93*, 073307.
(5) Morfa, A. J.; Rowlen, K. L.; Reilly, T. H.; Romero, M. J.; Van de Lagemaat, J. *Appl. Phys. Lett.* **2008**, *92*, 013504.
(6) Chen, F. -C.; Wu, J. -L.; Lee, C. -L.; Hong, Y.; Kuo, C. -H.; Huang, M. H. *Appl. Phys. Lett.* **2009**, *95*, 013305.
(7) Hayashi, S.; Kozaru, K.; Yamamoto, K. *Solid State Commun.* **1991**, *79*, 763–767.
(8) Kato, K.; Tsuruta, H.; Ebe, T.; Shinbo, K.; Kaneko, F.; Wakamatsu, T. *Mater. Sci. Eng., C* **2002**, *22*, 251–256.
(9) Mapel, J. K.; Singh, M.; Baldo, A.; Celebi, K. *Appl. Phys. Lett.* **2007**, *90*, 121102.
(10) Reilly, T. H., III; Lagemaat, J.; Tenent, R. C.; Morfa, A. J.; Rowlen, K. L. *Appl. Phys. Lett.* **2008**, *92*, 243304.
(11) Min, C.; Li, J.; Veronis, G.; Lee, J. Y.; Fan, S.; Peumans, O. *Appl. Phys. Lett.* **2010**, *96*, 133302.
(12) Diukman, I.; Tzabari, L.; Berkovitch; Tessler, N.; Orenstein, M. *Opt. Express* **2011**, *19*, A64–A71.
(13) Homola, J.; Koudela, I.; Yee, S. S. *Sens. Actuators B* **1999**, *54*, 16–24.
(14) Singh, B. K.; Hillier, A. C. *Anal. Chem.* **2006**, *78*, 2009–2018.
(15) Zeng, L.; Bermel, P.; Yi, Y.; Alamariu, B. A.; Broderick, K. A.; Liu, J.; Hong, C.; Duan, X.; Joannopoulos, J.; Kimerling, L. C. *Appl. Phys. Lett.* **2008**, *293*, 221105.
(16) Baba, A.; Kanda, K.; Ohno, T.; Ohdaira, Y.; Shinbo, K.; Kato, K.; Kaneko, F. *Jpn. J. Appl. Phys.* **2010**, *49*, 01AE02.
(17) Jiang, G.; Baba, A.; Advincula, R. *Langmuir* **2007**, *23*, 817–825.
(18) Baba, A.; Locklin, J.; Xu, R. S.; Advincula, R. *J. Phys. Chem. B* **2006**, *110*, 42–45.
(19) Baba, A.; Matsuzawa, T.; Sriwichai, S.; Ohdaira, Y.; Shinbo, K.; Kato, K.; Phanichphant, S.; Kaneko, F. *J. Phys. Chem. C* **2010**, *114*, 14716–14721.
(20) Ferry, V. E.; Munday, J. N.; Atwater, H. A. *Adv. Mater.* **2010**, *22*, 4794–4808.